International Journal of Multimedia and Ubiquitous Engineering
Vol.10, No.7 (2015), pp.237-246
http://dx.doi.org/10.14257/ijmue.2015.10.7.25

Exposing Image Sharpen Forgeries Based on Dyadic Contrast Contourlet

Hua Zhen and Li Jinjiang

Shandong Institute of Business and Technology, Yantai, China
huazhen66@foxmail.com

Abstract

In order to distinguish the sharpening operation in a manipulated image, a sharpen forgeries detection algorithm is proposed. Combined with efficient image signal processing method, a new non-subsampled dyadic contourlet transform based on contrast à trous wavelet is designed. In contourlet domain, sharpening characteristics are analyzed by multi-scale and multi-directional methods. A classifier is trained by artificial intelligence methods to complete sharpening tampered image detection. Experimental results show that the algorithm in this paper can detect possible sharpening and locate the tampering boundary accurately.

Keywords: *sharpened operation, image tampering, dyadic contourlet, contrast à trous wavelet*

1. Introduction

In today's Internet age, digital images become an important carrier of information, and more easily subject to tampering attacks. From the Photoshop to the light magic hand, the image tampering has increasingly become a popular entertainment, and its technical threshold has been lower, which led to the PS force is now overwhelming on the network. How to distinguish those images information has become an urgent problem to be solved. From the 2007 china's "South China Tiger" incident, the various incidents about photos forgeries have appeared. In addition to the network mode of explosion of information transmission behind this waves, it is also highlighted the helpless in the technical to the current image identification. Image as one of the important carrier of information, has been used in the media, the scientific assist and crime evidence and various aspects, if the images cannot guarantee it's truth, then no amount of follow-up is futile. In view of this, the image authentication technology has become a hot and difficulties research in the current image field.

Image authentication techniques can be divided into active and passive authentication according to the mode of certification [1]. Active Authentication refers to embed digital watermark or signature mark when the first image release, so in the future according to this tag to be quickly certified. However, active authentication technology in the front of current rapid development of technology of tampering has increasingly become little effect, faced with life difficulties. In this case, passive authentication technology becomes a flexible new option for people. Passive authentication technology is a blind forensics technology, without prior adjuvant treatment to the authentication image. It just need to get the image itself which be certified, and then can certification testing according to imaging principle and characteristics of the image which be altered at any time. Because certification image does not have any special requirements, it has the excellent operational and range of applications and prospects are more extensive, which has become the main direction of image authentication research. Hany distort the image into synthetic images, enhance image, variant images, retouching images, painting images and generated images

ISSN: 1975-0080 IJMUE

[2]. The most common way is cut the target of an image synthesis to another image, as well as make the fusion of synthesis of images look more natural, often through the sharpen operation or blur operation to the edge portion to make fake flawless.

In the current study of passive image authentication, the image tampering operation of the copy-paste, variants and computer-generated have more mature theory. However, as sharpened, blurred, graded, desalination and other polishing operation's flexibility and its uniform change in the frequency domain. For the operation of these tampered, the academic community don't have very accurate method of detection. Farid, Tsong, and Fridrich proposed the image synthetic tamper detection methods [3-7], but these methods for the image after retouch have little effective detection, China's Zhou Linna detected blur operator by edge characteristics of morphological filtering [8]. Wang use the rate of abnormal tone to detect the image blurs operation [9]. In this paper, combined with dyadic contrast contourlet, we proposed a blind detection algorithm for image tampering evidence according to the manifestations of the sharpen polish operation in the frequency domain. According to Experiments, the algorithm have an excellent recognition rate of image sharpening retouching operation, and have an effectively distinction between the artificial sharpened and nature image, accurate positioning of the splicing boundaries.

2. Dyadic Contrast Contourlet Transform

2.1. Dyadic Wavelet

Discrete Dyadic wavelet is a special case of wavelet framework, in which wavelet base function has characteristics of narrow band-pass filter, and also has properties of conservation of energy before and after the signal transform. Dyadic wavelet transform in time domain and space domain is continuous. It's only dyadic discrete on the scales, and translational of time domain remains continuous change. It has the same translation invariance with continuous wavelet transform, and can be effective to carry out image noise detection, localization and classification.

The follow definitions are given to describe the dyadic wavelet:

Definition 1. Function $\psi(t) \in L^2(R)$ is a one-dimensional dyadic wavelet, if has constant $0 < A \le B < \infty$ causes the equation below to be tenable:

$$A \le \sum_{j \in z} |\psi(2^j \omega)|^2 \le B \tag{1}$$

Definition 2. $\{\psi_1(x,y), \psi_2(x,y)\} \subset L^2(R^2)$ is a two-dimensional dyadic wavelet, if has constant $0 < A \le B < \infty$, causes the equation below to be tenable:

$$\forall \omega = \left(\omega_x, \omega_y\right) \in R^2 - \left\{\left(0,0\right)\right\} \tag{2}$$

$$0 < |\psi_1(2^j \omega_x, 2^j \omega_y)|^2 + |\psi_2(2^j \omega_x, 2^j \omega_y)|^2 \le B$$

In the above equation, $\hat{\psi}$ is the Fourier transform of ψ. The dyadic wavelet transform is defined as:

$$Wf(\mathrm{x},\mathrm{y}) = \left\{W_2^1 f(\mathrm{x},\mathrm{y}), \mathrm{W}_2^2 f(\mathrm{x},\mathrm{y})\right\}, j \in z \tag{3}$$

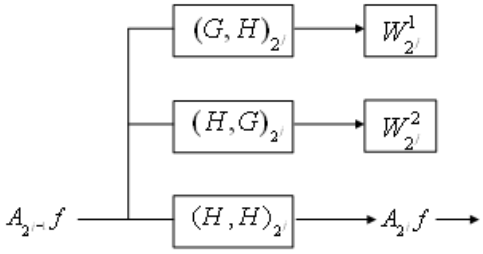

Figure 1. Dyadic Wavelet Decomposition

In the above equation, $W_2^1 f(x,y) = f(x,y) * \overset{-1}{\psi}_2(x,y)$,

$W_2^2 f(x,y) = f(x,y) * \overset{-2}{\psi}_2(x,y)$, and $\overset{-k}{\psi}_2(x,y) = (-x,-y), k = 1,2$.

The follow diagram is the decomposition of dyadic wavelet:

2.2. Dyadic Contrast Contourlet Transform

The traditional Contourlet transform adopt double contrast filter bank structure, and use contrast pyramid (CP) to decompose input signal to capture the singular point. It brought together near the singular point to a contour segment according to the direction information, thus completing the transformation steps.

CP decomposition is to generate a low-pass Gaussian pyramid of the target image as the low-pass copies of the target image. In the process of build the pyramid, every gradual decomposition of image can get by an "REDUCE" operation to generate the after image. "REDUCE" operation is the 5×5 window Gaussian average weighted operator of upper pixel. For each level of the pyramid ($1 < l < N$, N is the highest level of the pyramid), there are:

$$G_l = REDUCE(G_{l-1}) \tag{4}$$

As each layer of low-pass pyramid image's density and resolution are reduced, in the reconstruction of the prior level, interpolation to achieve through the "EXPAND" operation. Obviously, "EXPAND" operation is inverse operation of "REDUCE" operation. Defined the ratio low pass pyramid as follow:

$$\begin{cases} R_l = \dfrac{G_l}{EXPAND(G_{l+1})} & 0 \le l \le N \\ R_N = G_N \end{cases} \tag{5}$$

R_l is the ratio between adjacent levels of low-pass pyramid, so the ratio low-pass pyramid is a complete representation of the original target image. Its inverse can obtain the original target image. Luminance contrast defined as:

$$C = (L - L_b)/L_b = (L/L_b) - I \tag{6}$$

Where L is the brightness of the image in a specific location, L_b is the background brightness of the point. For any (i, j) , let $I(i, j) = 1$. Contrast pyramid defined as:

$$\begin{cases} C_l = \dfrac{G_l}{EXPAND(G_{l+1})} - I & 0 \le l \le N \\ C_N = G_N \end{cases} \tag{7}$$

C_l Sequence is a multi-scale decomposition of the target image get by the contrast pyramid, which decomposed the target image into several band-pass sub-band. You can use the reverse process to complete the reconstruction of the target image. Subsequently,

the high frequency sub-band obtained by CP decomposition using the direction filter banks (DFB) for the direction analysis [10].

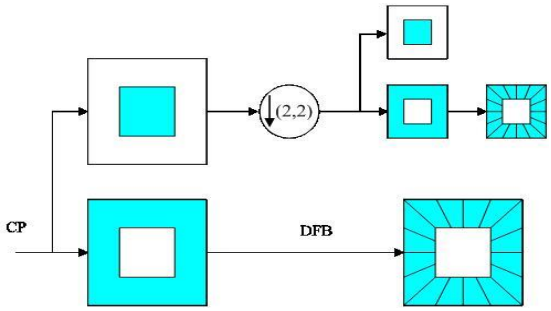

Figure 2. Dyadic Contrast Contourlet Transform

In order to change the traditional contrast Contourlet transfer's problems of lost translation invariance, spectral leakage and aliasing due to subsampling, we adopt tà trous wavelet algorithm to deal with dyadic wavelet which has non-subsampling characteristics to replace ratio low-pass pyramid of Contrast contourlet transform [11]. For the target image of evidence, we use à trous wavelet to generate approximate image sequence $p_l(l=1,2,\ldots \mathrm{N})$, where N is the number of layers of wavelet decomposition. We can define dyadic contrast à trous wavelet transform as follow:

$$\begin{cases} p_0 = p \\ w_l = (p_{l-1} / p_l) - I \quad 0 \le l \le N \\ w_N = p_N \end{cases} \tag{8}$$

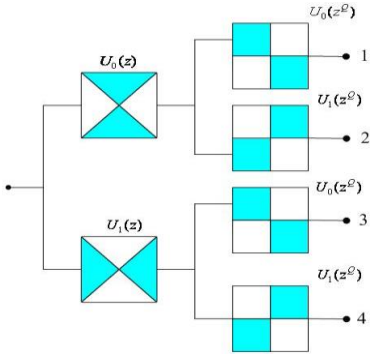

Figure 3. NSDFB Decomposition.

Similar to (7), for any (i, j), let $I(i, j)=1$. Accordingly, its inverse is the images reconstruction process. The directional analysis implement through Non-Subsampled Directional Filter Banks (NSDFB) [12]. NSDFB adopted a set of two-channel non-subsampled filter banks, decomposed in the direction of each layer, and then use all the filters of quincunx matrix $Q=\begin{pmatrix} 1 & 1 \\ 1 & -1 \end{pmatrix}$ top-sampled directional filter banks, which is the directional filter of next layer's directional decomposition. NSDFB decomposition schematic shown as Figure 3, $U(z)$ is filter.

So far, this paper on the basis of original Contourlet structure, construct a new non-subsampled dyadic contrast Contourlet transform. The main structural thinking is: first put forensic target image into dyadic contrast à trous wavelet transform; then put the high-frequency sub-bands obtained by the transform into NSDFB decomposition; low

frequency sub-band continue dyadic contrast à trous iterative after NSDFB decomposition. The overall process shown in Figure 4.

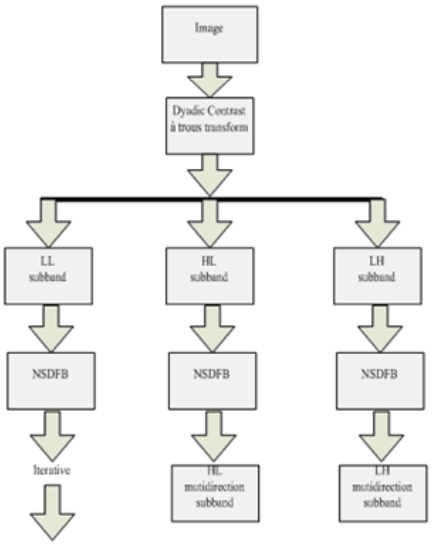

Figure 4. The Pre-Process of the Evidence Target Image

After the processing of the original evidence image signal, it have the multi-directional and frequency shift invariance, so the frequency domain information can be more fully utilized in the sharpen operation detection. With the use of the à trous dyadic wavelet, which is the "weapon" of signal amplification, we are able to trace any trace of the evidence target image, and greatly enhance the subsequent evidence operation's hit rate and accuracy. Decomposition as shown below, where Figure 5 is a sample image; Figure 6 is a dyadic contrast Contourlet transform's third level decomposition; Figure 7 is dyadic contrast Contourlet transform's decomposition of the fourth level.

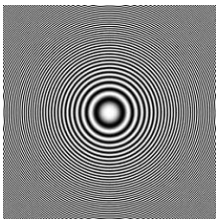

Figure 5. Sample Image

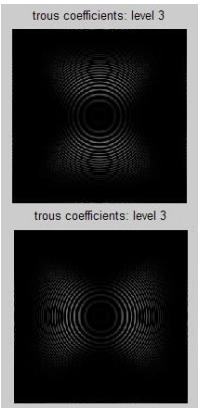

Figure 6. Transform's Third Level Decomposition

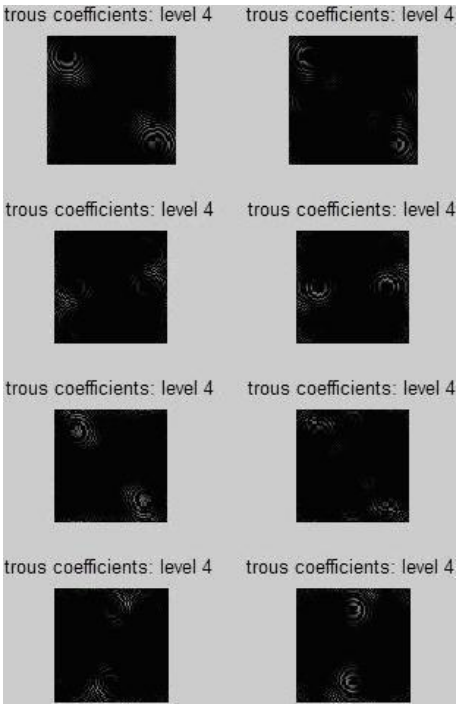

Figure 7. Transform's Fourth Level Decomposition

3. Amplification and Locating of the Sharpen Tampering

3.1. Extracted Sharpen Characteristics in Dyadic Contrast Contourlet Transform

The sharpening operation most significant reflected on the edge of the image, and therefore our analysis from the edge of the point to start. In the image, the edge point based on their strength classification is taken as a strong edge point. The less strong edge points and the weak edge point. Under normal circumstances, the distribution of these three edge point is found to a certain law. When image being sharpen tampering, the proportion of the three types of edge points will change significantly. Mainly due to weak edge points is enhance to the less strong edge points by sharpening tampering operation, the less stronger edge point is enhanced to strong edge points and with the sharpening intensity increased. In forensics algorithm by view of this, we get these three types of edge point detailed statistics and observations, the combination of the prediction error image, the characteristics of phase consistency, and the accurate positioning of the sharpening area.

For the image I which size is $m \times n$, in the three binary contrast contourlet decomposition, decomposition of each layer of the number of subbands are 8, here represented by Γ_a^b , (a is layer, b is subband component, $a = 1,2,3$; $b = 1,2,\ldots,8$). We make the following definition:

$$\Gamma_a(i, j)_{MAX} = \max(\Gamma_a^b(i, j)) \tag{9}$$

$\Gamma_a(i, j)_{MAX}$ represents a point (i, j) in the a layer, and the maximum is all 8 directional sub band component, $b = 1,2,\ldots,8$, $i = 1,2,\ldots, m$, $j = 1,2,\ldots, n$. Through the edge detection algorithm, we can get a set of edge points of the image I which is $E = \{e_{i,j} | 1 \le i \le m, 1 \le j \le n\}$. Strength of $e_{i,j}$ is not equal in the three dyadic contrast contourlet

decomposition. we can divide it into three sets: strong edge point set ES , the less strongest edge point set EM , weak edge point collection EW . We can get it and traverse the collection in accordance with the following rules elements, and placed in the corresponding collection:

(1)if $\Gamma_3(i,j)_{MAX} = \max(\Gamma_a(i,j)_{MAX})$, $a = 1,2,3$ then $e_{i,j} \in ES$;

(2) if $\Gamma_2(i,j)_{MAX} = \max(\Gamma_a(i,j)_{MAX})$, $a = 1,2,3$ then $e_{i,j} \in EM$;

(3) if $\Gamma_1(i,j)_{MAX} = \max(\Gamma_a(i,j)_{MAX})$, $a = 1,2,3$ then $e_{i,j} \in EW$;

After this step, we completed the classification of the image edge points, the distribution of point vary significantly between sharpening image and normal images, which can be used as a reference standard sharpening tampering forensics.

In order to more accurately position the sharpening tampering area, we can compare difference between the prediction error image and forensics target image [13]. When the image after sharpening retouch tampering, the error value will significantly increase, and we can put error image to dyadic contrast contourlet transform as a distinction of edge points' sharpening or not. Prediction error image can be expressed as $\Delta f = f - \hat{f}$, wherein f is the original image pixel value. $\hat{f}$ is the prediction image pixel value. The predicted pixel calculation method is:

$$\hat{f} = \begin{cases} \max(r,s), & if \quad t \le \min(r,s) \\ \min(r,s), & if \quad t \ge \max(r,s) \\ r+s-t, & \text{otherwise} \end{cases} \tag{10}$$

Wherein r, s, t is context pixels of the current pixel.

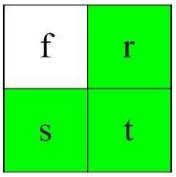

Figure 8. The Relationship of the Predict Pixels

After sharpening tampering, the edges of the image are substantially enhanced, and the phase coherence of its edge is more obvious than before the performance [14]. According to Fourier series in the phase characteristics of the points of various signals, it raised the phase consistency model, and the main features of the model are not the waveform to make any assumptions. In the transform domain to find one feature point in accordance with the phase-consistent sequence, its function can be expressed as:

$$C_2(x) = \frac{\sum_n U(x)\lfloor B_n(x)\Delta\Psi_n(x) - K \rfloor}{\sum_n B_n(x) + \xi} \tag{11}$$

In the above formula, $\Delta\Psi_n(x)$ is a phase shift function, expressed as:

$$\Delta\Psi_n(x) = \cos\left(\Delta\Psi_n(x) - \Delta\overline{\Psi}_n(x)\right) - \left|\sin\left(\Delta\Psi_n(x) - \Delta\overline{\Psi}_n(x)\right)\right| \tag{12}$$

Wherein $B_n(x)$ is the amplitude of the n scales, and $B_n(x)\Delta\Psi_n(x)$ represents a local energy function convolution obtained through the forensic image $I(x)$ and the log Gabor wavelet filter. ξ is a value of a very small constant and prevent the $\sum_n B_n(x)$ pole hour,

resulting in the expression does not stable. $U(x)$ is the weighting function of the filter band. K is the noise estimate energy, $\Psi_n(x)$ is the transform domain component of x at the n-th phase. $\Psi_n(x)$ represents the respective transform domain component in the formula (11), and takes a maximum value when the phase angle of the weighted average. We can calculate the prediction error image into phase coherence to obtain a targeted phase coherence FIG individually calculate the statistical collection edge point corresponding to this point in the phase coherence, and there 4 features for the collection of forensic image edge points: to the point of the center of the 3×3 neighborhood's mean, variance, skewness, and kurtosis. At this point, it is a combination of the first two reference standards, and a total of six reference standards as the basis to identify whether the image is tampered with after sharpening, which provides strong support for subsequent artificial intelligence methods on the tampered region's positioning.

3.2. Artificial Intelligence Methods to Position of the Sharpening Tampered Regions

With the previous sharpening distinguishing characteristic as a reference, we can use artificial intelligence methods to generate a lot of material accumulated experience classifier, and then use the experience classifier for forensics target image to detect sharpening tamper. As naive Bayesian method has the characteristic to build simple, fast computing. It has many advantages: loose coupling, noise immunity. The naive Bayes based attributes weighted classifier method [15] also overcome a simple shell that the Yates could easily lead to the assumption of independence distortion and range projections could easily lead to a decline in accuracy characteristics, so we chose to attribute weighted-based naive Bayes classification.

In the previous analysis, we put edge points divided into three cases to conduct research, when training the classifier. We use the classifier Bayes1 Bayes2 Bayes3 for these three kinds of edge points separate training. In training, the training samples are divided into two sets which are non-tampered images and tampered image training for the training. We selected 200 images, including grayscale and color images, and multiple categories of content, including figures, objects, buildings, landscapes, etc. The training for each sample as follows: Roberts operator edge detection point; then put this image and its prediction error image into dyadic contrast contourlet transform; accordance with the method of above section to place the edge points into ES, EM and EW collection; randomly select 20 each edge points from the three sets, then statistics the proportion of original and prediction error image's corresponding points of the component $\Gamma_3(i,j)_{MAX}$ of the of the expression of various types of edge point; calculate the consistency phase FIG of the error image, and selecting neighborhood of the edge point is located four statistical characteristics: the mean, variance, skewness, kurtosis, six training features for classifier training. After the completion of the original image training, this the 200 image uses two types of sharpening template sharpening tampering; then follow the training methods of the original image to tampered image training.

Table 1. The Statistics of Experiments

Source	*quantity*	*error quantity*	*correct quantity*	*correct rate(%)*
Cannon A720 original images	44	42	2	95.5
Cannon A720 tampered images	43	40	3	93
Non-tempered images form network	30	28	2	93
Tempered images form network	34	31	3	91.2
Kodak DC290 original images	37	34	3	91.8
Kodak DC290 tampered images	41	39	2	95.2

When classifier training completed, you will put forensics target image using a classifier to discriminate, and the determining point for sharpening edge for the corresponding marker to locate tampered area.

4. Experimental Results and Analysis

The algorithm execution environment is Matlab R2010a. The forensics target image source are from the tampered picture released on the network and the digital camera, in which original camera images using Photoshop CS4 for the artificial sharpening tampering retouching operations. The experimental results are shown in Figure 9. The first row of figure 9 is forensic image artificially splicing, by sharpening retouched so that splicing image appear more natural. The second row of figure 9 highlight an area of the image. From the experimental results, we can see how the pending the forensics image after feature extraction. After mature experience, using a classifier to recognize its sharpening region is more accurate positioning. In the experiment, we will be classified determines suspicious sharpening point edge points the highlight pixels calibration.

To verify the adaptability and robustness, as well as the distinction between original image and artificial sharpened, we collected from the digital camera, PS, and network spoof etc. a large number of sharpened images repeated the experiment, the results shown below：

As can be seen from the table, the algorithm can accurately identify and locate the image of artificial sharpened tampering. Image recognition for high-pixel camera is best. It is able to accomplish relatively accurate tampered evidence. For the network image, due to its altered approach more complex, the recognition rate dropped to a certain extent. So in the follow-up studies, it need to combine a variety of evidence means to improve the algorithm.

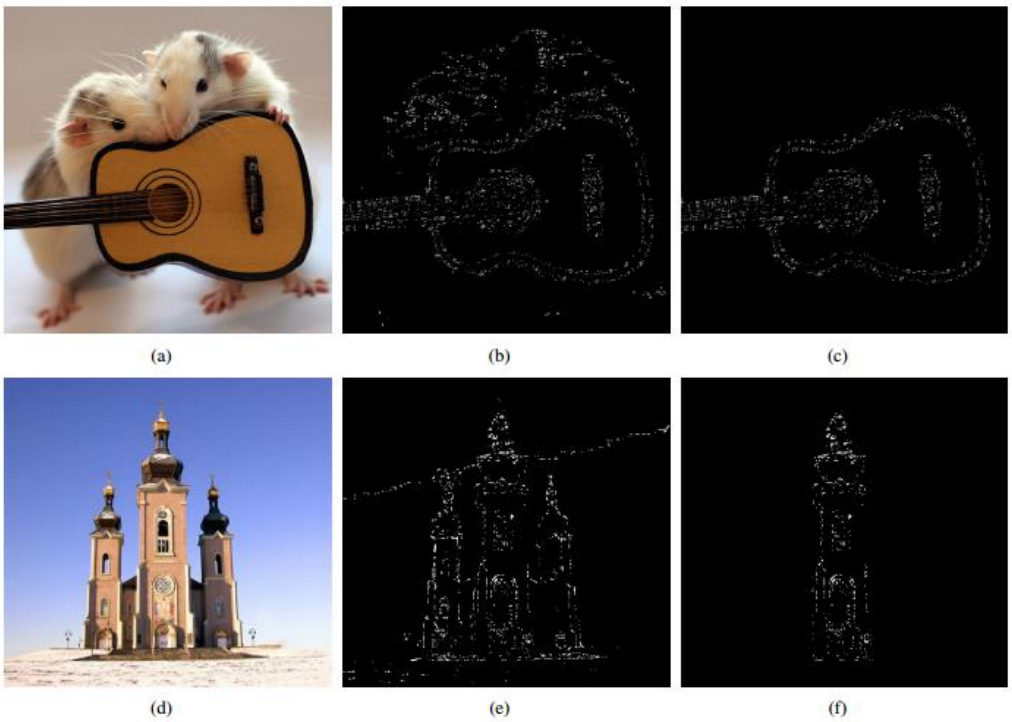

Figure 9. Experimental Results. (a) and (d) Are Input Image, (b) and (e) Are Edge Point, (c) and (f) Are Sharpening Region

5. Conclusions

In this paper, we use the features of artificial sharpen tampering image, combined with the signal processing methods in dyadic contrast Contourlet domain, provide a targeted evidence methods of the sharpened tampering image. The target evidence image first transform to a new domain of dyadic non-subsampled contourlet based on the contrast trous wavelet, then put it sharpening feature extraction. After AI classifier training, feature for forensics image is extracted in a dyadic contrast contourlet domain, and then determine whether the sharpening tampering picture by experienced classifiers. Experimental results show that this algorithm has better ability to identify artificial tampering image. Because the use of perfect signal processing methods in dyadic contrast Contourlet domain, image processing with more accurate positioning and refinement of the scale. For tampering image with the comprehensive means, the algorithm still have some shortcomings, and in future studies we should pay attention to evidence with a variety of means to improve the algorithm.

Acknowledgements

This work is supported by the National Natural Science Foundation of China under Grant No.61173173, 61272430, 61373079, 61472227. The Provincial Natural Science Foundation of Shandong under Grant No. ZR2013FM015.

References

[1] Lyu S., "Natural Image Statistics for Digital Image Forensics. Ph.D. dissertation," Department of Computer Science, Dartmouth College, **(2005)**.
[2] Hany F., "Creating and Detecting Doctored and Virtual Images: Implications to the Child Pornography Prevention Act. Ph.D. dissertation," Department of Computer Science, Dartmouth College, **(2004)**.
[3] Alin C. P. and Hany F., "Exposing digital forgeries by detecting duplicated image regions. Ph.D. dissertation," Department of Computer Science, Dartmouth College, **(2004)**.
[4] Tian T. N., Shih F. C. and Qibin S., "Detection of Photomontage Using Higher Order Statistics IEEE International Symposium on Circuits and Systems (ISCAS)," Vancouver, Canada, May 23-26, **(2004)**.
[5] Fridrich J., Soukal D. and Lukas J., "(Jan,2004). Detection of Copy move Forgery in Digital Images," Proceedings of Digital Forensic Research Workshop, Cleveland Ohio, USA, August 6-8, **(2003)**.
[6] Hsiao D. Y., "Detecting digital tampering by blur estimation," First International Workshop on Systematic Approaches to Digital Forensic Engineering. Taibei, China, November 7-9, **(2005)**.
[7] Tong H., "Blur detection for digital images using wavelet transform," International Conference on Multimedia Computing and Systems/International Conference on Multimedia and Expo – ICME (ICMCS), Taibei, China, June 27-30, **(2004)**.
[8] Zhou L., Wang D. and Guo Y., "Exposing digital forgeries by detecting image blurred mathematical morphology edge," Chinese Journal of Electronics, vol. 36 no. 6, **(2008)**, pp. 1047-1051.
[9] Wang B., Sun L. and Kong X., "Image forensics technology using abnormity of local hue for blur detection," Chinese Journal of Electronics, vol. 34 no. 12A, **(2006)**, pp. 2451-2454.
[10] M. N. Do and M. Vetterli, "The contourlet transform: an efficient directional multiresolution image representation," IEEE Transactions on Image Processing, vol. 14 no. 12, **(2005)**, pp. 2091-2106.
[11] Nunez J., Otazu X. and Fors O., "Multiresolution-Based Image Fusion with Additive Wavelet Decomposition," IEEE Trans. on Geosciences and Remote Sensing, vol. 37 no. 3, **(1999)**, pp. 1204-121l.
[12] A. L. Cunha, J. Zhou and M. N. Do, "The nonsubsampled contourlet transform: Theory, design and application," IEEE Transactions on Image Processing, vol. 15 no. 10, **(2006)**, pp. 3089-3101.
[13] Shi Y. Q. and Xuan G. T., "Image steg analysis based on moments of characteristic functions using wavelet decomposition, prediction-error and neural network," International Conference on Multimedia Computing and Systems, Dhaka, Bangladesh, December 28-30, **(2005)**.
[14] Kovesi P., "Image feature from phase congruency," Journal of Computer Vision Research. vol. l no. 3, **(1999)**, pp. 1-27.
[15] Webb G. I. and Pazzan J., "Adjusted Probability Naïve Bayesian induction," Proceedings of the Eleventh Australian Joint Conference on Artificial Intelligence, Brisbane, Australia, July 13–17, **(1998)**.

